

# A study on how top-surface morphology influences the CO<sub>2</sub> storage capacity

Anne Randi Syversveen, Halvor Møll Nilsen, Knut-Andreas Lie, Jan Tveranger, and Petter Abrahamsen

**Abstract** The primary trapping mechanism in CO<sub>2</sub> storage is structural trapping, which means accumulation of a CO<sub>2</sub> column under a deformation in the caprock. We present a study on how different top-seal morphologies will influence the CO<sub>2</sub> storage capacity and migration patterns. Alternative top-surface morphologies are created stochastically by combining different stratigraphic scenarios with different structural scenarios. Stratigraphic surfaces are generated by Gaussian random fields, while faults are generated by marked point processes. The storage capacity is calculated by a simple and fast spill-point analysis, and by a more extensive method including fluid flow simulation in which parameters such as pressure and injection rate are taken into account. Results from the two approaches are compared. Moreover, by generating multiple equiprobable realisations, we quantify how uncertainty in the top-surface morphology impacts the primary storage capacity. The study shows that the morphology of the top seal is of great importance both for the primary storage capacity and for migration patterns.

---

Anne Randi Syversveen  
Norwegian Computing Center, PO Box 114, Blindern, N-0314 Oslo, Norway, e-mail: Anne.Randi.Syversveen@nr.no

Halvor Møll Nilsen  
SINTEF ICT, PO Box 124, Blindern, N-0314 Oslo, Norway, e-mail: hnil@sintef.no

Knut-Andreas Lie  
SINTEF ICT, PO Box 124, Blindern, N-0314 Oslo, Norway, e-mail: Knut-Andreas.Lie@sintef.no

Jan Tveranger  
Center for Integrated Petroleum Research, Uni Research, PO Box 7800 N-5020 Bergen, Norway, e-mail: Jan.Tveranger@uni.no

Petter Abrahamsen  
Norwegian Computing Center, PO Box 114, Blindern, N-0314 Oslo, Norway, e-mail: Petter.Abrahamsen@nr.no

## 1 Introduction

Whether CO<sub>2</sub> can be stored in saline aquifers and abandoned reservoirs is mainly a question of costs and the risk associated with the storage operation; most of the technology required to inject CO<sub>2</sub> is already available from the petroleum and mining industry. If a potential storage operation is to be feasible, the storage capacity of the site must be sufficiently big, one must be able to inject CO<sub>2</sub> at a sufficient rate without creating a pressure increase that may threaten the caprock integrity, and the overall probability for leakage during and after the injection must be acceptable.

The need to provide confident assessments of maximum injection rates, storage capacity, and long-term behaviour of injected CO<sub>2</sub> has led to the development of comprehensive numerical simulation capabilities (see e.g., [2, 3]), which in turn, however, has nurtured an often lopsided emphasis on numerical- and modelling-based uncertainties in this area of research [3, 7]. Uncertainties from formation properties have received less attention: Academic studies of CO<sub>2</sub> injection frequently employ simplified or conceptualised reservoir descriptions in which the storage formation has highly idealised geometry and is considered nearly homogeneous. Geological knowledge and experience from petroleum production, however, show that the petrophysical characteristics of potential CO<sub>2</sub> sequestration sites can be expected to be heterogeneous on the relevant physical scales, regardless of whether the target formation is an abandoned petroleum reservoir or a pristine aquifer. Complex geology introduces tortuous subsurface flow paths, baffles, and barriers, which in turn influence reservoir behaviour during injection. It is important that the effect of geological heterogeneity is quantified by the research community. This will facilitate both improved understanding of subsurface flow at operational CO<sub>2</sub> injection sites, and allow comparison with simulated flow in ideal homogeneous models and upscaled versions of these.

A key challenge when assessing the impact of heterogeneity is to quantify the uncertainty associated with the precise spatial structure of formation properties. To provide a statistically sound frame of reference for understanding the behaviour of injected CO<sub>2</sub> in subsurface formations, several sedimentological scenarios need to be evaluated. Moreover, multiple geostatistical realisations of each sedimentological scenario are required to quantify the relative effect of uncertainties associated with depositional and structural architecture and their associated petrophysical properties. In this paper, we will study how uncertainty in top-surface morphology may impact estimates of primary storage capacity as well as migration patterns.

## 2 Geological modelling

Geological heterogeneity influences fluid movement in the subsurface and occurs at all scales. Most geological parameters used for describing reservoir-type rocks (e.g., mineralogy, grain-size, grain shape, sorting, cementation, sedimentary structures, bed-thickness) express heterogeneity at often very fine scales. Physical properties of

the rock are linked to these descriptive geological parameters and their scale through direct measurement, empirical databases, or established physical relationships (e.g., pore-size, pore shape, pore throat diameter, connectivity, elasticity, shear strength).

In reservoir models, heterogeneity is commonly expressed as spatial distribution of porosity and permeability on the scale dictated by model resolution. It follows that heterogeneity at scales below model resolution is treated either implicitly, by considering the cell sizes of the model as common representative elementary volumes (REV) for all features in the model, or alternatively derived from more detailed models through upscaling. In both cases, simplification of existing heterogeneity is the rule, highlighting the importance of keeping scale considerations in mind when dealing with geological heterogeneity. Mapping out the impact of geological features on CO<sub>2</sub> sequestration would therefore ideally require a study covering all possible types of geological features, how to upscale them and charting their effect on fluid flow through a series of simulation studies. The scale of such an effort is beyond the scope of any single project or the capacity of any single group, but it should certainly form a clear goal and ambition for a collective research effort.

Being a buoyant fluid, CO<sub>2</sub> moves up from the point it is being injected until encountering a barrier that prevents further upward or lateral movement. At this point, the fluid will move laterally upslope along the barrier until it either reaches the end of the barrier or a closure/trap where accumulation can take place. As the trap fills, it may either overspill, causing further lateral migration of CO<sub>2</sub>, or experience pressure build-up to a point where trap integrity may be compromised and seal bypass occurs, at which point CO<sub>2</sub> will intrude into the seal and leak into the overlying formation. It follows that the morphology of the interface between the reservoir and overlying seal will affect CO<sub>2</sub> migration pathways, shape, and size of local accumulations as well as the evaluation of seal integrity on reservoir scale. To investigate these effects, a series of generic scenarios were defined which included depositional and structural features affecting top-reservoir morphology in a synthetic reservoir model measuring 30 × 60 km<sup>2</sup>. The scale of the features included was constrained by the 100 × 100 × 5 m<sup>2</sup> resolution of the model.

For depositional features, two scenarios were chosen for which it was considered likely that a depositional/erosional topography could be preserved under a thick regional seal; the latter commonly formed by marine shale. The two scenarios reflect situations where sand deposition in an area similar to the model size is succeeded by deposition of fines as a result of marine transgression:

1. Offshore sand ridges covered by thick marine shale (OSS)
2. Preserved beach ridges under marine shale (FMM)

Generic input for the scales and geometries of the two scenarios was compiled from published literature on recent and ancient offshore sandbanks and drowned beach ridges. Input data are summarised in Table 1.

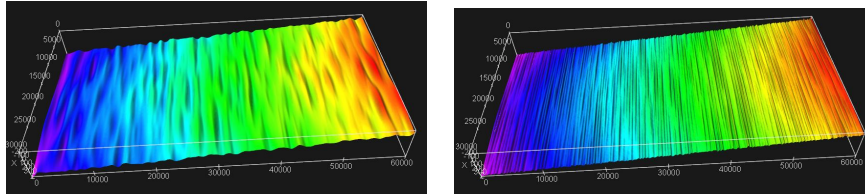
In addition to the preserved depositional topography, a series of conceptual structural scenarios were generated with fault patterns extending over the entire model area. The scenario details are listed in Table 2.

**Table 1** Morphometric data for preserved topographic features (offshore sand ridges, OSS and flooded marginal marine, FMM) capped by the top seal.

Scenario label	OSS	FMM
Amplitude	<20 m	1–10 m
Width	2–4 km	10–300 m
Length	10–60 km	<15 km
Spacing	2–4 km	40–300 m

**Table 2** Geometric definitions of fault populations for the four faulted reservoir scenarios.

Scenario label	UP1	NP1	UP2	NP2
Displacement	uniform; 100 m	random; 20–150 m	uniform; 100 m	random; 20–150 m
Length	uniform; 4000 m	random; 300–6000 m	uniform; 4000 m	random; 300–6000 m
Strike	uniform; 90°	uniform; 90°	30° and 90°	30° and 90°

**Fig. 1** Top surfaces: the left plot shows offshore sand ridges (OSS) and the right plot shows a flooded marginal marine (FMM) deposition.

### 3 Stochastic modelling

Once geological base-case scenarios are defined, their intrinsic uncertainty can be explored using geostatistical methods. Factors that affect the behaviour of the injected CO<sub>2</sub> in the reservoir include the morphology of the overlying seal, presence of barriers like sealing faults and reservoir porosity, and permeability distribution. To explore the impact of top-seal morphology, a set of top reservoir surfaces were generated by superimposing different sinusoidal structures, reflecting the geological features to be modelled, onto a base-case surface. The shape of the base-case surface was chosen so as to keep the injected CO<sub>2</sub> plume within the model area. It has the shape of an inverse half-pipe parallel to the longest axis of the model, with a 500 m height difference over a distance of 60 km. This corresponds to a gradient of 0.48 degrees, which is low, but not unrealistic, for basins of this size.

The top surfaces of the OSS and FMM models were created by Gaussian random fields. A sinusoidal variogram of form  $\sin(x)/x$  was used for both models. For OSS, the range was 1000 m along the long axis and 7000 m along the short axis with

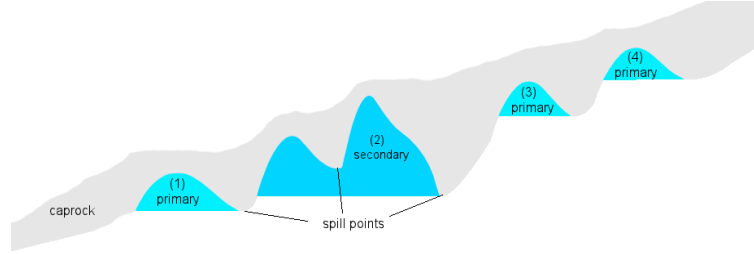


**Fig. 2** Illustration of the calculation of spill points upslope of an injection point. In the cascade of structural traps, a primary trap has no interior spill point, secondary trap has one interior spill point, and so on.

standard deviation equal 13 m. For the FMM case, the range along the long axis was 200 m and 7000 m along the short axis with standard deviation equal 5 m. One realisation of each model is shown in Figure 1. Faults were generated by the fault modelling tool HAVANA [4], which is based on a marked-point model. For UP1 and UP2, we use strong repulsion to get uniformly distributed faults and a small variance for the fault length to have constant length. In NP1 and NP2, the fault length has a larger variance, and the repulsion between faults is weaker.

Variations in reservoir porosity and permeability have so far not been considered, but are important heterogeneity factors that should be investigated at a later stage.

#### 4 Flow simulation and estimation of structural trapping

To quantify the impact of changing geological parameters, we will consider a simple scenario in which CO<sub>2</sub> is injected from a single point (injection well). Chief among the immediate concerns during CO<sub>2</sub> injection are primarily pressure build-up during injection, and secondly storage capacity and migration of injected CO<sub>2</sub>. The topography of the top surface is unlikely to have significant impact on pressure build-up during injection, and thus our attention will be focused towards storage capacity and CO<sub>2</sub> migration.

As a simple estimate of fluid migration, we will use a spill-point calculation [1] in which fluid is injected at an infinitesimal rate and the buoyant forces dictate flow. Such calculations are extremely fast, and allow the full model suite to be quickly assessed in terms of maximum upslope migration distance for a given injection volume from a specific injection point. A slightly more advanced analysis is achieved by identifying the cascade of all structural traps associated with a given top-surface morphology, defined so that primary traps contain a single local peak, secondary traps contain one saddle-point and more than one peak, tertiary traps contain two saddle-points, etc, see Figure 2. Using this cascade of traps, one can bracket the potential for structural trapping, estimate structural trapping for finite injection rates, optimise placement of injection points, etc.

When CO<sub>2</sub> is injected at a finite rate, it will form a plume that may move too fast in the upslope direction to be able to fill all structural traps predicted by the spill-point analysis. Likewise, the plume will also spread in the transverse direction and possibly contact other structural traps that cannot be reached by the spill-point algorithm. A full 3D simulation of the high-resolution stochastic models is not possible, at least not with the commercial and in-house simulators we have available. Instead, we will use a reduced model based upon vertical integration of the two-phase flow equations, see e.g., [6, 5]. Since we are mainly concerned with the long-term migration, the implied time-scales make the assumption of vertical segregation and equilibrium a robust choice from the perspective of upscaling.

## 5 Results

Using the setup presented in the previous sections, we have conducted a study of how top-surface morphology affects structural and residual trapping and to what extent the CO<sub>2</sub> plume is retarded during its upslope migration.

*Example 1 (Structural trapping).* In the first example, we will study how the top-surface morphology affects capacity estimates for structural trapping. To study the impact of geological uncertainty, we generate one hundred realisations of each of the fifteen model scenarios (except for the flat, unfaulted scenario, for which only a single realisation is needed). For each realisation, we computed the total volume available to residual trapping based upon the cascade of structural traps described in the previous section. Table 3 reports the mean volumes for a uniform porosity of 0.25 with uncertainty specified in terms of one standard deviation. In the table, the structural complexity increases from left to right and the complexity of the sedimentary topography increases from top to bottom.

**Table 3** The total volume available for structural trapping for the fifteen different types of top-surface morphologies. The table reports mean volumes in 10<sup>6</sup> m<sup>3</sup> and one standard deviation estimated from one hundred realisations for each scenario assuming a porosity of 0.25.

	unfaulted	UP1	NP1	UP2	NP2
Flat	0 ± 0	96 ± 5	74 ± 23	79 ± 5	50 ± 14
OSS	608 ± 122	648 ± 99	715 ± 120	639 ± 115	629 ± 118
FMM	227 ± 22	278 ± 21	314 ± 38	260 ± 20	259 ± 27

For the flat depositional topography, all structural traps are fault traps. Here, the fault patterns with all faults normal to the flow direction (UP1 and NP1) give larger volumes than the cases that have additional faults with a strike angle of 30° relative to the flow direction (UP2 and NP2). This reduction in volume depends critically on how effective the faults that are not parallel to the trapping structure are at limiting

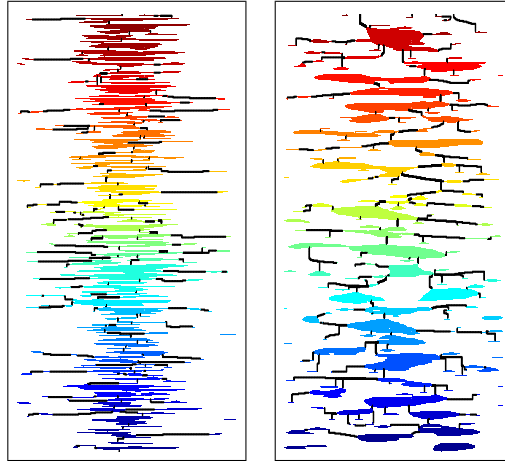


**Fig. 3** The cascade of structural traps for FMM UP1 (left) and OSS UP1 (right). In the plots, the traps are presented in a tree structure with black lines denoting spill paths connecting traps in the upslope direction. Colours are used to distinguish different traps (numbered in the upslope direction).

their trapping volume. As expected, we also observe a larger uncertainty in each fault pattern when introducing a random length and displacement.

For the unfaulted cases, all structural traps are fold traps induced by the depositional topography. Here, the case with offshore sand ridges (OSS) has significantly larger storage capacity, mainly because the fold traps have lobes with larger amplitude, width, and length. Compared with the flat cases, we see that the volumes in the fold traps are (almost) one order of magnitude larger than the volumes in the fault traps.

For the cases having a combination of fold and fault traps, faults normal to the flow direction increase the storage capacity, in particular for the flooded marginal marine (FMM) cases. On the other hand, faults having a strike angle of 30° relative to the upslope direction will open some of the fold traps and hence lead to a (slightly) lower structural trapping capacity. Because the OSS scenarios have fewer and larger lobes, the variation between different realisations is larger than for the FMM cases. This is illustrated in Figure 3, which shows the cascade of traps and how they are connected through spill paths for two specific cases; traps that are not connected will form different trees. We see that the OSS case gives trees with more branches, while the FMM case has more nodes in the biggest tree.

The study reported in Table 3 only considers potentially favourable injection scenarios in which lobes in the depositional topography are orthogonal to the upslope direction. Rotating the lobes (and the fault strikes) ninety degrees resulted in very small structural trapping capacity.

*Example 2 (Single injector).* In practise, it will be very difficult to utilise all the potential storage volume that lies in the structural traps unless one is willing to drill and

operate a large number of injection wells. To get a more realistic estimate of actual trapping in a plausible injection scenario, we perform a spill-point calculation with a fixed injection point at coordinates (15, 15) km. Table 4 reports the corresponding mean trapped volumes with an added uncertainty of one standard deviation. Figure 4 shows structural traps computed for one realisation of each of the fifteen scenarios.

**Table 4** Trapped volumes in units of  $10^6 \text{ m}^3$  computed by a spill-point analysis with a single source at coordinates (15, 15) km.

	unfaulted	UP1	NP1	UP2	NP2
Flat	$0 \pm 0$	$20 \pm 5$	$30 \pm 19$	$13 \pm 3$	$15 \pm 12$
OSS	$419 \pm 123$	$431 \pm 153$	$441 \pm 180$	$404 \pm 153$	$379 \pm 141$
FMM	$239 \pm 24$	$268 \pm 24$	$278 \pm 94$	$175 \pm 25$	$184 \pm 45$

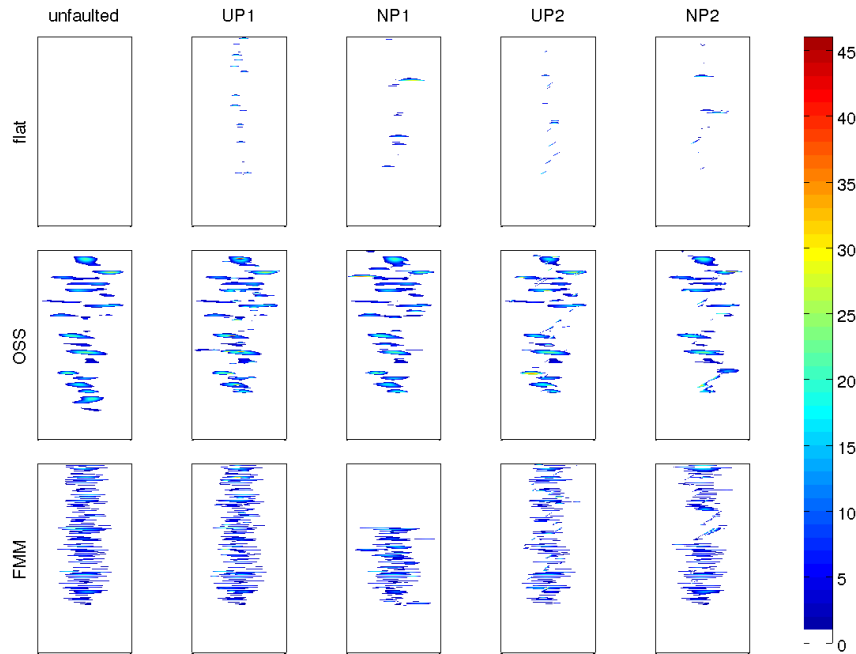


**Fig. 4** Height in meters inside structural traps computed by a spill-point analysis. The columns show different structural scenarios and the rows different depositional scenarios.

As expected, the spill-point analysis predicts that only a fraction of the structural traps will be filled with  $\text{CO}_2$ . For the preserved beach ridges (FMM), the spill-point and total volumes are almost the same for the unfaulted cases and the cases with

no crossing fault. Here, the lobes in the top-surface morphology are narrow, tightly spaced, and relatively long in the transverse direction, which means that the CO<sub>2</sub> will spread out laterally before migrating upslope. This observation is confirmed by the FMM-unfaulted and FMM-UP1 cases in Figure 4, where we see that the spill path connects with almost all traps in the middle of the formation. In some of the FMM-NP1 cases—e.g., the one shown in the figure—leakage over the edges prevents the injected CO<sub>2</sub> from reaching the top. The actual trapped volume will therefore be much smaller than the total capacity of the whole top surface. Leakage over the edges also explains why the variation in Table 4 has increased significantly compared with Table 3 for some of the OSS and FMM scenarios. If cases with leakage are disregarded, the variation in volumes becomes more similar to the variation seen in Table 3. For crossing faults, the faults having a strike angle of 30° will accelerate the upslope migration of CO<sub>2</sub> and reduce the lateral filling, see the FMM-NP2 case in Figure 4. As a result, the spill-point analysis predicts that approximately 67% and 71% of the available volume will be filled. For offshore sand ridges, the spill-point analysis predicts a filling degree of 60–69%. Because the fold traps are much larger than for the FMM cases, spill paths may miss large traps on their way to the top.

For the flat cases, the spill path resulting from a single injection point will only contact a few of the available fault traps, and hence the analysis predicts that only 16–40% of the available volume is filled for the particular injection point chosen herein. For cases having only fault traps, a much better injection strategy would thus be to use an array of injectors to improve the utilisation of structural trapping.

Next, we will study how our estimates of structural trapping depend upon the placement of the injection point. To this end, we pick one specific realisation for each scenario as shown in Figure 4 and consider fifteen different injection points placed on a regular mesh with nodes at  $x = 5, 10, \dots, 25$  km and  $y = 10, 15, 20$  km. Table 5 reports the corresponding trapping volumes calculated by a spill-point analysis. As observed in the previous example, the variation in volumes is significantly larger for the cases with offshore sand ridges than for the flooded marginal marine cases.

**Table 5** Volumes in units  $10^6$  m<sup>3</sup> from spill-point calculations with varying placement of the injection point.

	unfaulted	UP1	NP1	UP2	NP2
Flat	0 ± 0	21 ± 2	32 ± 3	11 ± 2	19 ± 11
OSS	311 ± 94	366 ± 121	340 ± 106	317 ± 48	250 ± 75
FMM	272 ± 21	276 ± 20	182 ± 24	208 ± 17	196 ± 22

*Example 3 (Prediction by flow simulation).* We continue with the set of fifteen realisations used in Example 2 and a single well at (15, 15) km injecting at a rate of one million cubic meters per year. For simplicity, the reservoir is assumed to be homo-

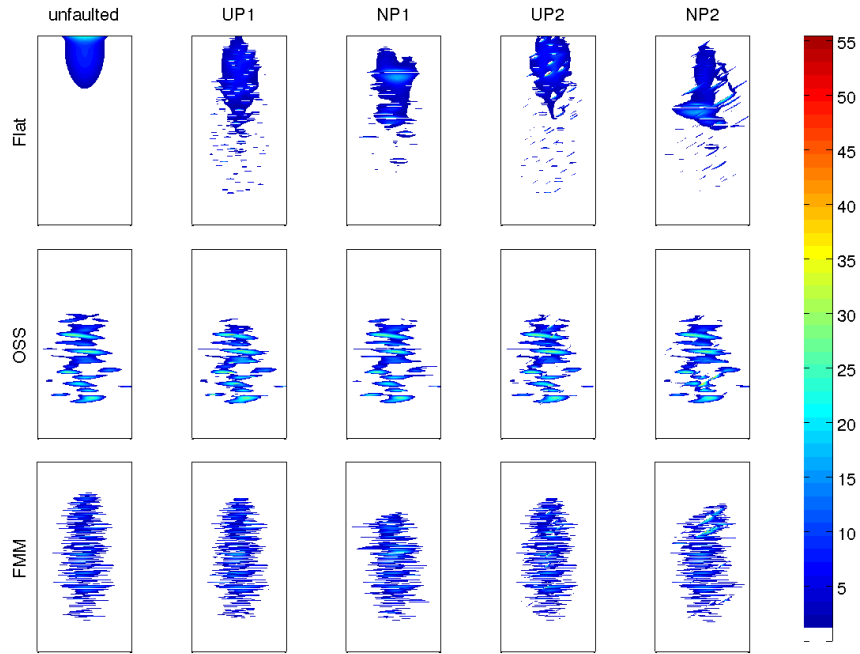


**Fig. 5** Height in meters for the plumes of free CO<sub>2</sub>. The columns show different structural scenarios and the rows different depositional scenarios.

geneous, with an isotropic permeability of 500 milli Darcy. Table 6 shows the free and residually trapped volumes computed by a flow simulation using a vertically-integrated model. The free volume is defined as the volume that is not residually trapped and includes volumes confined in fold and fault traps. At a first glance, the volumes for all the different scenarios may seem surprisingly similar and it may appear counter-intuitive that the residual trapping is largest for the flat cases. However, for cases with a flat deposition there is (almost) no relief in the top-surface morphology that will retard the plume migration. Hence, the plume will either reach or come very close to the top of the model within a migration period of 5000 years (see Figure 5), and in the process sweep a relatively large volume, which results in large volumes of residually trapped CO<sub>2</sub>. For the scenarios with offshore sand ridges, on the other hand, the large lobes in the top surface will force the upslope migration of the injected CO<sub>2</sub> to predominantly follow ridges in the morphology, which retard the plume migration and reduce the residual trapping compared with the flat scenarios. The FMM cases are somewhere in between. We also observe that having faults of varying length (NP1 and NP2) retards the plume migration slightly compared with cases having uniform faults (UP1 and UP2).

With regard to structural trapping, the situation is completely different. Here, OSS has the largest volumes, as seen in Table 7, while the flat scenarios have almost no structural trapping, even in the faulted cases. Comparing FMM and OSS, we see

**Table 6** Free and residually trapped volumes in units of 10<sup>6</sup> m<sup>3</sup> computed by a flow simulation with a vertically-integrated model and a single injection point at (15, 15) km.

	unfaulted		UP1		NP1		UP2		NP2	
Flat	214	297	248	263	248	263	238	273	263	248
OSS	355	156	365	146	357	153	357	154	360	151
FMM	300	211	304	207	315	196	305	206	305	206

that the OSS scenarios have approximately 50% more structurally trapped CO<sub>2</sub>. To compare structural trapping predicted by flow simulation and by spill-point analysis, we note that in the flow simulation, the CO<sub>2</sub> plume has not reached the top of the structure after 5000 years for the OSS and FMM cases. The spill-point calculations, on the other hand, are run until the top is reached and hence overestimate the structurally trapped volumes. Conversely, for the flat depositional scenario, the spill-point analysis predicts a thin CO<sub>2</sub> trail that only contacts a few fault traps, whereas in the flow simulations the injected CO<sub>2</sub> plume spreads laterally and therefore contacts more fault traps, and hence gives higher trapped volumes.

**Table 7** Comparison of structurally trapped volumes in units of 10<sup>6</sup> m<sup>3</sup> computed by spill-point analysis and by simulation with a vertically-integrated model.

	unfaulted		UP1		NP1		UP2		NP2	
Flat	0	0	22	34	31	20	11	24	16	27
OSS	324	150	370	164	352	150	315	158	250	141
FMM	276	111	289	101	183	115	209	93	205	95

The volume of movable CO<sub>2</sub> is obtained by subtracting the structurally trapped volume from the free volume. A surprising result is that the movable CO<sub>2</sub> volume is approximately the same for all of the models and represents between 39% and 45% of the total injected volume. In terms of risk, however, quoting only the movable percentage is quite misleading. For the flat deposition, almost all the movable CO<sub>2</sub> volume has accumulated close to the upslope boundary. The OSS and FMM cases, on the other hand, show different degrees of retention and hence the probability of leakage will also vary a lot. For the OSS cases, most of the movable CO<sub>2</sub> is still far from the boundary and will gradually become structurally and residually trapped. Here, the CO<sub>2</sub> plume also moves very slowly since it is forced to cross the spill points decided by the top-surface morphology. The FMM cases appear somewhere between the OSS and the flat cases, and here the plume moves a bit further because it 'feels' less effects from the top-surface morphology in the beginning of the migration when the height of the plume is larger than the height of the sand ridges.

## 6 Concluding remarks

CO<sub>2</sub> is affected by top-reservoir morphology. However, the spread of the CO<sub>2</sub> plume is only inhibited if the height of the plume is of the same scale as the amplitudes of the relief. For low injection rates, a modest relief may slow migration, whereas for high injection rates creating a thick plume, the effect is negligible. Spill-point calculations are fast, but capture only structurally trapped CO<sub>2</sub>. A large number of realisations can be run quickly using flow simulations based upon a vertically-integrated formulation, thereby allowing a fast way of measuring volumetric uncertainty of CO<sub>2</sub> retention. More comprehensive simulation results will be presented in a forthcoming paper.

Our study highlights the necessity of including geological detail to models forecasting realistic CO<sub>2</sub> migration. The manner in which these elements affect migration must be understood, which calls for new modelling initiatives in which more detailed geology is considered.

## References

1. Abrahamsen, P., Hauge, R., Heggland, K., Mostad, P.: Uncertain cap rock geometry, spillpoint and gross rock volume. In: Proceedings from SPE Annual Technical Conference and Exhibition. SPE49286, New Orleans, Louisiana (1998)
2. Celia, M.A., Nordbotten, J.M., Bachu, S., Kavetski, D., Gasda, S.: Summary of princeton workshop on geological storage of CO<sub>2</sub>. Princeton-bergen series on carbon storage, Princeton University (2010). Uri: <http://arks.princeton.edu/ark:/88435/dsp01jw827b657>
3. Class, H., Ebigbo, A., Helmig, R., Dahle, H.K., Nordbotten, J.M., Celia, M.A., Audigane, P., Darcis, M., Ennis-King, J., Fan, Y., Flemisch, B., Gasda, S.E., Jin, M., Krug, S., Labregere, D., Beni, A.N., Pawar, R.J., Sbai, A., Thomas, S.G., Trenty, L., Wei, L.: A benchmark study on problems related to CO<sub>2</sub> storage in geologic formations. *Comput. Geosci.* **13**(4), 409–434 (2009). DOI 10.1007/s10596-009-9146-x
4. Hollund, K., Mostad, P., Nielsen, B.F., Holden, L., Gjerde, J., Contursi, M.G., McCann, A.J., Townsend, C., Sverdrup, E.: Havana — a fault modeling tool. In: A.G. Koestler, R. Hunsdale (eds.) Hydrocarbon Seal Quantification. Norwegian Petroleum Society Conference, 16–18 October 2002, Stavanger, Norway, *NPF Special Publication*, vol. 11. Elsevier (2002)
5. Ligaarden, I.S., Nilsen, H.M.: Numerical aspects of using vertical equilibrium models for simulating CO<sub>2</sub> sequestration. In: Proceedings of ECMOR XII–12th European Conference on the Mathematics of Oil Recovery. EAGE, Oxford, UK (2010)
6. Nordbotten, J.M., Celia, M.A.: Geological Storage of CO<sub>2</sub>: Modeling Approaches for Large-Scale Simulation. Wiley (2012)
7. Pruess, K., Garca, J., Kovscek, T., Oldenburg, C., Rutqvist, J., Steefel, C., Xu, T.: Code inter-comparison builds confidence in numerical simulation models for geologic disposal of CO<sub>2</sub>. *Energy* **29**(9–10), 1431–1444 (2004). DOI 10.1016/j.energy.2004.03.077